

Impact of photo-oxidation technology on the aqueous solutions of nitrobenzene: Degradation efficiency and biodegradability enhancement

Fares Al Momani*

Chemical Engineering Department, Mutah University, Karak, Jordan

Received 22 March 2005; received in revised form 17 July 2005; accepted 12 August 2005

Available online 17 October 2005

Abstract

Advanced oxidation processes (AOPs) using photo-Fenton treatment was investigated at laboratory scale for the degradation of aqueous solutions of nitrobenzene (from now on NB). The effects of reactants concentration, temperature and pH on nitrobenzene degradation were monitored. Photo-Fenton treatment was successfully led to abate the NB in the aqueous solution. At pH 3, and with initial concentrations of 65 mg L^{-1} for H_2O_2 and 10 mg L^{-1} for Fe(II), the photo-Fenton treatment degraded all the nitrobenzene (initial NB concentration of 100 mg L^{-1}) in only 30 min. The effect of initial concentration of Fe(II) catalyst on degradation efficiency and biodegradability was followed. Fe(II) showed moderate effect in the degradation of NB and small effect on the biodegradability improvement. Increasing the initial iron ion concentrations from 10 to 50 mg L^{-1} was led to increase in the degradation efficiency from 75 to 90%, and was led to increase BOD_5 from 13 to $16 \text{ mg O}_2 \text{ L}^{-1}$. Biodegradability and acute toxicity of the treated solutions was investigated. Experimental results showed a considerable increase in treated solution biodegradability and reduction in acute toxicity as a result of the photo-Fenton processes. BOD_5 was increased from 0 for untreated solution up to $34 \text{ mg O}_2 \text{ L}^{-1}$ at the point where all NB was eliminated from the solution, meanwhile toxicity unit TU was decreased from 25 to 8 at the same elimination efficiency.

© 2005 Elsevier B.V. All rights reserved.

Keywords: Nitroaromatic; Oxidations; Reagent concentrations; Toxicity

1. Introduction

Nitroaromatic compounds are commonly used in the manufacture of pesticides, dyes and explosives. As a result of its wide use, these compounds are often detected in industrial effluents, ambient freshwater, ambient environments and atmosphere [1]. The presence of these nitroaromatics compounds in different types of water effluent causes a threat to human health and produces a public concern. Recently, the US EPA have been listed them among the 130 priority pollutants to be investigated in the period 2001–2005 [2,3]. One of the main ways of contamination of superficial wastewaters by nitroaromatic compounds are the residual industrial effluents. The studies performed by Refs. [4,5] have reported the presence of nitroaromatics substances in surface waters and ground waters. The concentrations of

nitroaromatic compounds in industrial effluents were reported elsewhere [5].

Among nitroaromatic compounds, nitrobenzene is most common pollutant. Nitrobenzene is readily soluble in most organic solvents and is completely miscible with diethyl ether and benzene [6]. It is a good solvent for aluminum chloride and is therefore used as solvent in Friedel–Craft reactions. It is slightly soluble in water (0.19% at 20°C ; 0.8% at 80°C). Nitrobenzene is released into the environment primarily from industrial uses but it can also be formed in the atmosphere by the nitration of benzene, a common air pollutant. The largest sources of nitrobenzene release are from its high use as primary chemical intermediate in the synthesis of aniline. Smaller amounts are also released from products in which nitrobenzene is used as a solvent. Nitrobenzene can also evaporate if exposed to air. Once evaporated in air, nitrobenzene breaks down to other chemicals. In USA, the most releases of nitrobenzene to environment are to underground injection sites. Available information indicates that nitrobenzene is moderately toxic to aquatic life. Nitrobenzene

* Tel.: +962 32372384; fax: +962 32372384.
E-mail address: fares1233@mutah.edu.jo.

Nomenclature

A	frequency factor
BOD_5	5 days biological oxygen demand [$\text{mg O}_2 \text{ L}^{-1}$]
COD	chemical oxygen demand ($\text{mg O}_2 \text{ L}^{-1}$)
$[NB]$	concentration of nitrobenzene at any time [mg L^{-1}]
$[NB]_i$	initial concentration of nitrobenzene [mg L^{-1}]
$[H_2O_2]_i$	initial concentration of H_2O_2 [mg L^{-1}]
$[Fe(II)]_i$	initial concentration of $Fe(II)$ [mg L^{-1}]
$[TOC]$	total organic carbon concentration [mg C L^{-1}]
$[TOC]_i$	initial total organic carbon concentration [mg C L^{-1}]
% TOC	% total organic carbon elimination
EC_{50}	effective concentration at which 50% reduction in bacterial light emission during the Microtox [®] toxicity bioassay
TU	toxicity unit
% NB	nitrobenzene degradation efficiency (%)
E	activation energy (kJ/mol)
R	ideal gas constant (8.314 J/(mol K))
T	temperature (K)

may be stored in plants, but it is not expected to accumulate in fish. Nitrobenzene has high toxicity to human being, it can provoke serious health problems, e.g. blood dyscrasia, eyes and skin irritations, and affect the central nervous system [7].

Studies on the stability of nitrobenzene in water has been estimated that its half-life varies from 1 day for natural channels to 3.8 days in aerated lagoons [8,9]. As nitrobenzene in aqueous form does not bind well to soil, it can move through the ground and enter ground water. In surface water, nitrobenzene was detected in only 0.4% of surface water and in 1.8% of reporting stations on industrial wastewaters. Furthermore, the presence of nitrobenzene in municipal wastewaters in a concentration between 20 and 100 mg L^{-1} has been detected.

Previous studies have demonstrated that traditional physical and chemical treatment technologies, such as coagulation, precipitation and adsorption on activated carbon [10], ultra-filtration and nano-filtration [11] and activated sludge [12] can be used efficiently to remove some constituents from wastewater and/or reduce the effluent toxicity. However, these processes are considered as non-destructive since they merely transfer those constituents from the liquid phase to the solid phase. Consequently, the regeneration of the adsorbent material and post-treatment of solid wastes, which are expensive operations, are still needed [13].

In the last decay, different chemical treatment processes was proposed as efficient treatment option for organic contaminant removal. One promised treatment is the use of high oxidizing capacity obtained from different advanced oxidation processes (AOPs) configurations [14,15]. AOPs are advantageous over other conventional treatment processes for a number of reasons: (1) they are destructive processes which do not transfer contaminants from one phase to another; (2) they can oxidize

contaminants in a short period of time; (3) they can be conducted at ambient temperatures; (4) the primary catalysts (e.g. iron and titanium) for these AOPs are non-toxic, readily available and relatively inexpensive [16–19]). Among AOPs, O_3 , UV/H_2O_2 , $UV/Fe(II)$, Fenton and photo-Fenton processes are capable of oxidizing a wide range of contaminants [20–22]. Understanding the chemical oxidation process is very important theme, from both theoretical and practical point of view, for achieving higher treatment levels. With the proper operational and kinetic data effective process control, appropriate design and economical capital and operational cost can be achieved [23,24].

In this study, the photocatalytic degradation of nitrobenzene was studied. The objectives was to investigate the effect of different photo-Fenton operational conditions on the degradation of aqueous solutions of nitrobenzene, and consequently, improvement in the treated solution biodegradability, follow the evolution of treated solution toxicity, tabulate optimum operation conditions and tabulate kinetic data for high nitrobenzene removal rate and better biodegradability.

2. Materials and methods

2.1. Installation

The experiments were done in an experimental device, whose scheme is shown in Fig. 1. The photochemical installation consists of (1) mixing tank at which a NB solution of 100 mg L^{-1} was prepared with water. The solutions were perfectly mixed to guarantee that all NB was dissolved, and the required concentrations of iron salt $FeSO_4 \cdot 7H_2O$ were added when necessary, (2) continuous stirred tank (CSTR) water jacket photo-reactor equipped with black light blue lamp, placed at its center. This lamp emits radiation basically at 360 nm. The nominal power of the lamp is 12 W. The solution mixing was performed via magnetic bar and base agitator. The reaction temperature in the CST reactor was maintained at a pre-set temperature achieved by water circulation in thermostatic water bath, and (3) neutralization tank. This tank was used to neutralize the treated solution if required. Peristaltic pumps were used to transfer the solutions from one tank to the other.

The light intensity entering to the photo-reactor was measured periodically (each 100 irradiation hours) by chemical actinometry. The actinometry is based on the photochemical

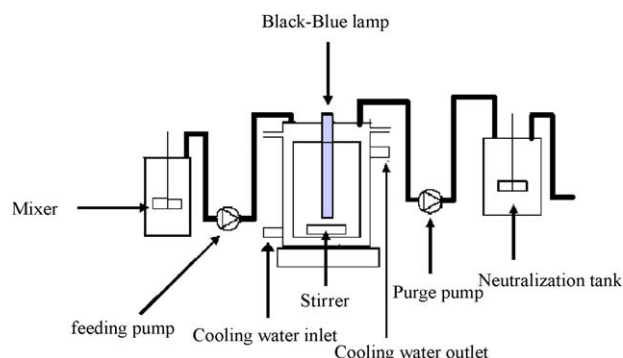
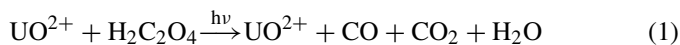


Fig. 1. Photo-chemical installation.

decomposition of oxalic acid (0.05 M) in the presence of uranyl nitrate (0.01 M). The reaction mechanism is complicated, and many products seem to be produced, like CO, CO₂, CHOOH, U⁴⁺ and H₂O [25,26]. Thus, for a pH value in the range of 3 and 7, oxalic acid conversions should be controlled to be lower than 20%. Under these conditions, the main reaction that takes place is:



The general actinometrical procedure and mathematical treatment for the used photo-reactor is explained in Ref. [27].

For a wavelength of 360 nm, the system quantum yield was equal to 0.51 mol Einstein⁻¹. Through the actinometry, the radiation fluxes entering the reactor, at the beginning and end of photo-Fenton experiments, were 4.5 ± 0.5 and 3.9 ± 0.5 μEinstein s⁻¹, respectively.

2.2. Procedure

All the experiments were carried out in batch mode and a starting solution pH in the range of 3–11. In each experiment, a NB and iron solution were prepared with water. After that, the photo-reactor was filled with the solution and was mixed for 5 min. A 30% aqueous hydrogen peroxide solution was injected into the reactor at different initial concentrations and the UV-light was switched on at the same time. During the experiments, samples were withdrawn from the reactor at several time intervals (0, 5, 10, 20 and 30 min), tested for H₂O₂ consumption with Quantofix test sticks and quenched with sodium hydrogen sulphite to avoid further reactions. The withdrawn samples were used later for TOC analysis. The reaction final solutions was used for the biological oxygen demand test (BOD) after being neutralized and part of it was used as formed for chemical oxygen demand test (COD).

2.3. Reagent

Nitrobenzene (>98%, Merck), H₂O₂ (30%, Merck), iron sulphate 7-hydrate FeSO₄·7H₂O (98%, Panreac), sodium hydrogen sulphite solution (40%, w/v, Panreac), potassium permanganate (99%, Probus), acetonitrile (99.8%, isocratic grade for HPLC, Merck), phosphoric acid (85.5%, Probus), potassium dichromate (99%, Probus), mercury sulfate (98%, Probus), silver sulfate (98%, Probus) and sulfuric acid (95–98%, Fluka).

2.4. Analytical methods

Nitrobenzene concentration was determined by reverse-phase high performance liquid chromatography (HPLC). HPLC analysis was performed with a Shimadzu liquid chromatograph (Shimadzu Scientific Instruments) equipped with Shimadzu pumps (model LC-10 AT) and a Shimadzu UV-vis detector (model SPD-10A). The reverse-phase column used was a C₁₈ μ Bondapak, (3.9 mm i.d. × 300 mm length, Waters). The mobile phase was a mixture of water and acetonitrile (65:35%) isocratically delivered by a pump at a flow rate of 1 mL min⁻¹. For the

UV-vis detector, the wavelength of the UV absorbance was set at 277 nm. Under these conditions, the retention time for NB was 13 min. To assure reasonable measurements, the standard solution and the tested concentration measurements was repeated for five times, obtained results were averaged, tested and gave as a maximum 5% standard deviation of the mean value.

The dissolved organic carbon was measured using a TOC analyzer, provided with an auto-sampler and using potassium phthalate solution as the calibration standard. For data reproducibility, each sample was tested three times and averaged, the average value was used in preparing the figures. Thus, it was observed that the precision in TOC measurements were in the range of ±1 mg CL⁻¹.

BOD was measured according to the procedures explained in Standard Methods [28] (1985) section 5210D. An Oxitop system (VELP Scientifica) was used. The bacteria used in this test were obtained from the activated sludge system, operating at municipal wastewater treatment plant. The precision in BOD test was in the range of ±1.5 mg O₂ L⁻¹. It is known that bio-oxidation is a slow process and theoretically takes long time to go to completion [7]. Within 21-day period 99% complete, and in 5-day period used for the BOD test. Oxidation ranges from 60 to 70%. However, during this study, BOD₂₁ was tested periodically; no significant increment was noticed between BOD₁₀ and BOD₂₁. Hence, it was decided to present only the data related to BOD₁₀ and BOD₅.

Chemical oxygen demand (COD) was carried out via a photometer (LF 2400, windows labortechnik) using dichromate solution as oxidant, in strong acid media [28] section 5220D. The precision in COD test was in the range of ±1.5 mg O₂ L⁻¹.

2.5. Toxicity analysis

Toxicity bioassays were performed on the treated solutions to evaluate the effect of pre-treatment process toxicity of treated solutions. The tests were carried out using Microtox[®] bioassays, which involves the use of a marine bacterium *Photobacterium phosphoreum* as an indication of sample toxicity. During the test, the bacterium emits light as a result of normal metabolic processes, and the light was measured with a Model 500 photodetection analyser. Toxicity was measured by the decrease in light intensity, which was directly linked to the presence of substances that interfere with metabolic activities of the bacterium. The effect of light reduction was evaluated for various sample dilutions, and linear regression of the results allowed for the determination of the EC₅₀ of the sample. EC₅₀ is the concentration of test sample at which there is a 50% reduction in bacterial light production. Thus, EC₅₀ values were inversely proportional to toxicity, lower EC₅₀ value relates to a more toxic sample. In order to eliminate dealing with inverse relationships, EC₅₀ values were converted to toxicity units (TU) using the following equation:

$$\text{TU} = \frac{100}{\text{EC}_{50}} \quad (2)$$

where TU is the toxicity unit and EC₅₀ is the concentration of test sample at a 50% reduction in bacterial light production.

Sample toxicity was evaluated at 5 and 15 min from the time of mixing at various dilutions with the bacterium. Procedures followed standard Microtox protocol and data analysis was achieved using the Microtox™ Omni Software (SDI, 2002).

3. Result and discussion

3.1. Photo-Fenton degradation of NB solution

The degradation efficiency of photo-Fenton on aqueous solution of nitrobenzene was studied. Four different set of experiments were performed; in each set of experiments, one operating parameter was varied, meanwhile the other parameters were kept the same. For example, photo-Fenton reaction was performed under different initial concentrations of H_2O_2 , while the initial Fe(II) concentration, solution pH and reaction time were unvaried.

Fig. 2 relates the evolution of NB concentration as a function of reaction time at different initial hydrogen peroxide concentration. At initial hydrogen peroxide concentration of 10 mg L^{-1} , the concentration of NB in the solution was decreased, during the 30 min irradiation time, from 100 to 68 mg L^{-1} . Higher initial hydrogen peroxide led to more NB oxidation. Total NB elimination was obtained when the initial hydrogen peroxide concentration of 65 mg L^{-1} was used. The Fe(II) initial concentration and irradiation time were 10 mg L^{-1} and 30 min, respectively.

Fig. 3 shows the degradation efficiency and organic carbon elimination of NB solution, obtained during different experiments, treated with different initial H_2O_2 concentration. Points in Fig. 3 represent the average of several experiments (at least two) carried out in the same operational conditions. As before, increasing the initial concentration of H_2O_2 was led to increase in the degradation efficiency of NB. As initial concentration of hydrogen peroxide increase from 10 to 55 mg L^{-1} , NB degradation efficiency was increased, during the 30 min irradiation time, from 48 to 95%. The solution pH was 3 and initial concentration of Fe(II) was 10 mg L^{-1} . It was expected during photo-Fenton reaction, increasing the initial hydrogen peroxide will increase the degradation efficiency to point where the reaction

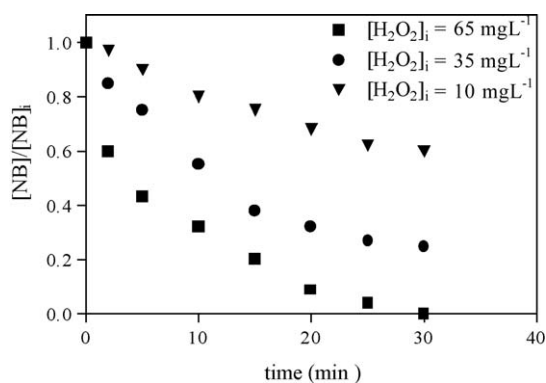


Fig. 2. Evolution of NB concentration as a function of reaction time at different initial hydrogen peroxide concentrations. $[\text{Fe}(\text{II})]_i = 10 \text{ mg L}^{-1}$, 30 min irradiation time and pH 3.

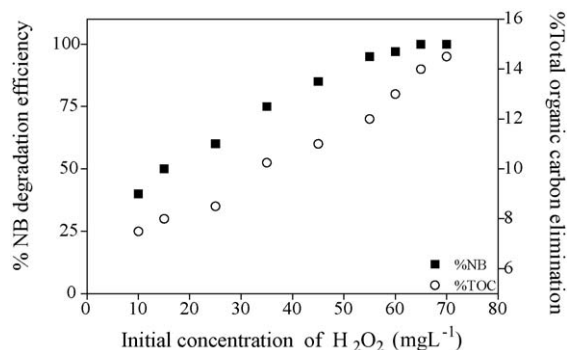


Fig. 3. NB degradation efficiency and total organic carbon elimination as function of initial H_2O_2 concentration. $[\text{Fe}(\text{II})]_i = 10 \text{ mg L}^{-1}$, 30 min irradiation time and pH 3.

efficiency level off (hydrogen peroxide might act as hydroxyl radicals scavenger). This tendency would be used to determine the optimum hydrogen peroxide concentration. Nonetheless, in our experiments, this effect was not seen. Increasing the initial H_2O_2 concentration more than 55 mg L^{-1} was led to increase the degradation efficiency. Thus, it was decided to stop the photo-Fenton reaction at the point where 100% elimination of the contaminant (NB in this case) occurs. The corresponding initial H_2O_2 concentration for total NB removal was 65 mg L^{-1} .

It is known that H_2O_2 has a maximum absorbance at 210–230 nm and NB takes maximum absorbance at 277 nm, these wavelengths fall a way of the wavelength of the used UV lamp (360 nm). This type of lamps was used, in this work, to the following reasons:

1. H_2O_2 proteolysis can take place to a small limit at wavelength $\approx 360 \text{ nm}$ (Pignatello et al., 1999). This was also noticed in the present work.
2. The spectrum of NB shows maximum absorbance at 277 nm. But, it has a significant absorbance up to 360 nm. This can be reason for its effective degradation efficiency in the present work.
3. Iron photo-redox is known to take place under high wavelength UV-light $\approx 360 \text{ nm}$.
4. From economical point of view, the use of cheap black blue lamp, compared with the expensive high pressure mercury lamp (254 nm), enhance the treatment feasibility.

The total organic carbon (TOC) elimination was also followed during NB degradation. Experimental results showed that increasing NB elimination efficiency led to increase the TOC % elimination, at the point where all NB was eliminated a 14% of TOC elimination was achieved.

The pre-treated solutions, 5 and 10 days biological oxygen demand (BOD_5 , BOD_{10}) was followed. Fig. 4 illustrates BOD_5 and BOD_{10} as function of initial H_2O_2 used in photo-Fenton reactions. Both values were increased substantially (from zero value), for pure NB solution, by increasing the initial concentration of H_2O_2 . Being 34 and $39 \text{ mg O}_2 \text{ L}^{-1}$ for BOD_5 and BOD_{10} , respectively, at H_2O_2 initial concentration of 65 mg L^{-1} (concentration needed to eliminate all NB). An increase in the BOD_5

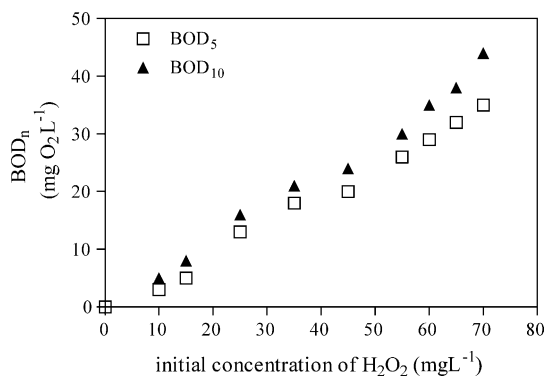


Fig. 4. The effect of initial H₂O₂ concentration on BOD₅/COD and BOD₅/TOC ratios. [Fe(II)]_i = 10 mg L⁻¹, 30 min irradiation time and pH 3.

of a sample due to the pre-treatment would indicate enhancement of biodegradation capability. At the light of the experimental results, it can be concluded that in terms of biodegradability, photo-Fenton is a proper pre-treatment process.

Other important parameter in photo-Fenton process is the concentration of Fe(II). Fig. 5 presents the influence of different Fe(II) initial concentration on NB degradation efficiency and organic carbon elimination. Experiments were conducted with fixed H₂O₂ initial concentration of 35 mg L⁻¹, pH of 3 and reaction time of 30 min. Although, in the previous section, maximum NB degradation efficiency was obtained at initial hydrogen peroxide concentration of 65 mg L⁻¹. In this section, it was decided to use initial H₂O₂ concentration of 35 mg L⁻¹. The reasons behind that were: (1) initial H₂O₂ concentration of 65 mg L⁻¹ may consider as high oxidation reagent concentration which affects the feasibility of the process negatively. (2) The study aims to optimize the initial concentrations of chemical reagents (H₂O₂ and Fe(II)) and to increase the NB degradation efficiency. Thus, lower initial reagents concentration is recommended. (3) If in this section, 65 mg L⁻¹ of initial H₂O₂ concentration was used, it will be difficult to follow the contaminant concentration (NB) throughout the oxidation process (at 65 mg L⁻¹ initial H₂O₂ concentration and only 10 mg L⁻¹ Fe(II) NB degradation efficiency was 100%). Fig. 5 shows that increasing Fe(II) initial concentration was led to degrade more NB until it reach to point at which no effect of added Fe(II) amount observed. This fact may attribute to two reasons: (1) high initial Fe(II) concentra-

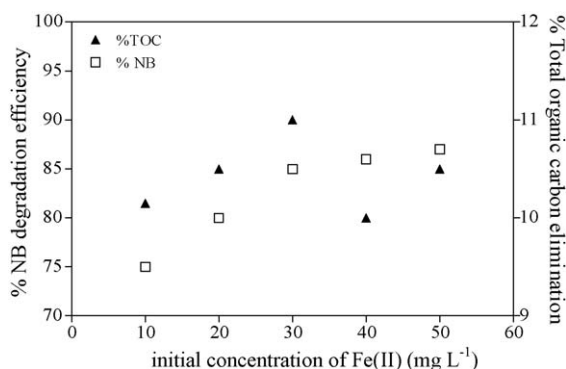


Fig. 5. Effect of initial concentration of Fe(II) on the degradation efficiency of NB. [H₂O₂]_i = 35 mg L⁻¹ 30 min reaction time and free pH evolution.

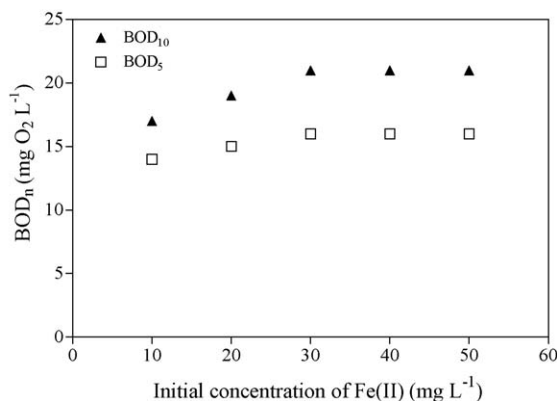


Fig. 6. Evolution of BOD₅ and BOD₁₀ as function of initial Fe(II) concentrations. [H₂O₂]_i = 30 mg L⁻¹, 30 min reaction time and initial pH 3.

tion produced brown turbidity in reaction solution that causes the recombination of hydroxyl radicals [29] and (2) iron ion Fe(II) can react with the present hydroxyl radical as a scavenger [30,31].

With respect to total organic carbon elimination, Fig. 5 shows that under all initial Fe(II) concentrations, % TOC was in the same order of magnitude, being the maximum 11%. The low total organic carbon elimination behaviour could be explained by the same hypothesis as that used to account for NB degradation efficiency (recombination of hydroxyl radicals and iron ion scavenging).

The effect of Fe(II) initial concentration on biological oxygen demand of the treated solution was also investigated. Fig. 6 presents the evolution of 5 and 10 days biological oxygen demand as function of initial concentrations of Fe(II) used. Unlike the H₂O₂, increasing the Fe(II) initial concentration does not lead to considerable increase in biodegradability. As initial concentrations of Fe(II) increased from 10 to 50 mg L⁻¹, BOD₅ increased from 13 to 15 mg O₂ L⁻¹, respectively.

Table 1 illustrates the effect of operational temperature on degradation efficiency of NB and solution BOD. It can be noted from these data, at all experimental conditions studied, there was a modest trend indicating a significant increase in the degradation efficiency with increasing operational temperature. The degradation efficiency increased from 75 to 90% by increasing the temperature from 25 to 45 °C. This was in agreement with what one might speculate, since it stands to reason that a higher temperature would increase the chemical oxidation rate.

Table 1 also presents the effect of oxidation reaction temperature on treated solution BOD. Experimental data illustrates that increasing reaction temperature was led to considerable enhancement on the solution biodegradability. As

Table 1
Results for the degradation of NB at different temperatures

T (°C)	% NB	% TOC	BOD ₅ (mg O ₂ L ⁻¹)	BOD ₁₀ (mg O ₂ L ⁻¹)
25	75	10	18	21
35	83	12.5	25	29
45	90	13	34	38

[H₂O₂]_i = 35 mg L⁻¹; [Fe(II)]_i = 10 mg L⁻¹; 30 min irradiation time; pH 3.

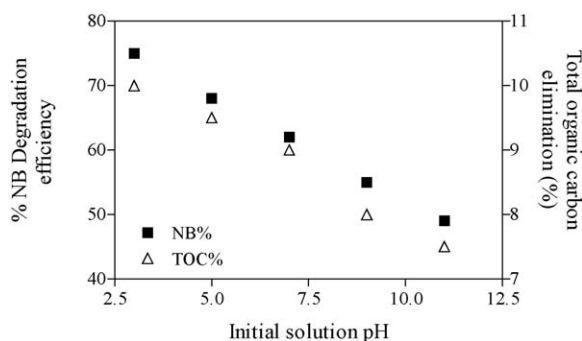


Fig. 7. Influence of initial solution pH in the degradation of NB. $[\text{H}_2\text{O}_2]_i = 35 \text{ mg L}^{-1}$, $[\text{Fe}(\text{II})]_i = 10 \text{ mg L}^{-1}$ and 30 min reaction time.

the temperature increased from 25 to 35 °C, BOD_5 increased from 18 to 34. Similar tendency was observed in BOD_{10} values.

The previous experiments were performed with initial solution pH of 3. For practical treatment operation, it is interesting to obtain data on the effect of initial treated solution pH variation on both degradation efficiency and BOD. Fig. 7 presents the NB degradation efficiency and total organic carbon elimination as a function of initial solution pH. Results indicate that the degradation efficiency is related to the initial solution pH, increasing the initial solution pH was led to decrease in both degradation efficiency and total organic carbon elimination. As the initial solution pH increased from 3 to 11, degradation efficiency was decreased from 70 to 49%. The final solution of photo-Fenton reaction pH was measured for these experiments; it was found that no matter of the initial starting pH, the final solution pH was decrease to a value of 3. This finding may explain the observed tendency, which means that photo-Fenton reaction does not start in forming hydroxyl radicals before the solution pH reach acidic condition. Moreover, it was noticed with experiments carried out at alkaline pH ($\text{pH} > 8$) that the aqueous solution colour change as the reaction proceeds to completion. This fact can be attributed to the dissolution of iron hydroxide as the solution pH decrease. This fact was clear for experiments carried out at high initial iron concentration $> 30 \text{ mg L}^{-1}$. However, no significant iron precipitation was noticed due to low initial Fe(II) concentration used and fast oxidation reaction kinetic which decrease the treated solution pH to acidic conditions.

The same effect was observed on solution BOD; increasing the initial solution pH was led to small enhancement in the treated solution BOD (result not shown).

If organic matter oxidation in photo-Fenton process were held in a highly oxidative environment, all the contained organic matter can be mineralized to CO_2 and water. Photo-Fenton process was tested to mineralize 100 mg L^{-1} NB solutions. The mineralization was followed by measuring the total organic carbon reduction in the treated solution. As photo-Fenton degradation efficiency affects by different conditions (e.g. reactants concentration, reaction time, temperature and pH) and based on the previous results, it was decided to perform the experiments at initial solution pH of 3, room temperature (25 °C), for practical purpose and extend the reaction time to 240 min. Fig. 8

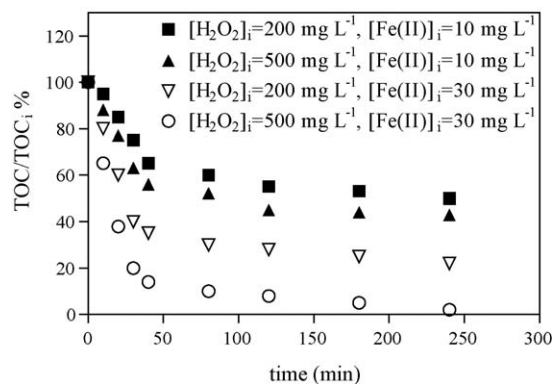


Fig. 8. TOC reduction as function of reaction time for 100 mg L^{-1} NB. Initial solution pH 3 and temperature = 25 °C.

presents the TOC reduction as function of reaction time at different initial concentrations of H_2O_2 and Fe(II). Photo-Fenton reaction could be used effectively for total NB mineralization. A hydrogen peroxide initial concentration of 500 mg L^{-1} and initial concentration of Fe(II) of 30 mg L^{-1} was sufficient to eliminate all the contained organic matter.

3.2. Toxicity analysis

Raw and pre-treated samples were tested using Microtox[®] bioassays. The effect of treated sample on acute toxicity was assessed by evaluating the correlation between residual toxicity and the fraction of NB degraded. Fig. 9 illustrates the relationship between the fraction of NB reduced and the residual toxicity. It was noticed that the pre-treatment of NB produced by-products with lower toxicity compared to that of untreated sample. There was a direct relation between the degradation efficiency of NB and the toxicity value. At maximum NB degradation efficiency (100%), the TU was reduced from 25 for untreated NB sample to 8 for the treated sample. Similar tendency was observed in experiments carried out at different operational conditions in terms of reduce on the toxicity as function of NB degradation efficiency.

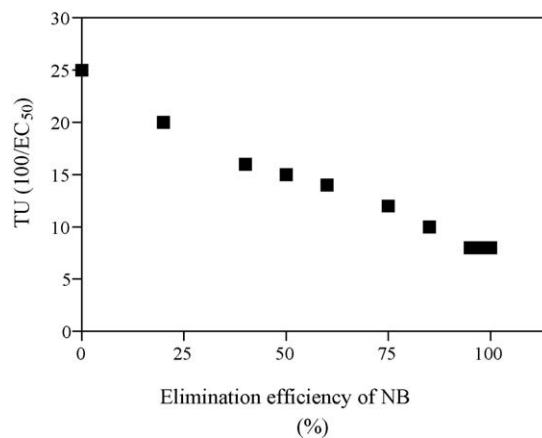


Fig. 9. Decrease in toxicity of NB solution as a function of degradation efficiency. $[\text{H}_2\text{O}_2]_i = 35 \text{ mg L}^{-1}$, $[\text{Fe}(\text{II})]_i = 10 \text{ mg L}^{-1}$, pH 3 and 30 min reaction time.

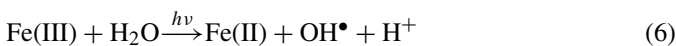
3.3. Kinetic perspectives

For theoretical and practical application, it is important to understand the oxidation kinetics of the treatment process. Reasonable kinetic data can produce optimum reactor design, efficient treatment process with good control, economical capital investment and operational cost. Fig. 2 presents some of kinetic data related to NB oxidation, the decay in NB concentration throughout the oxidation experiment is an indication of oxidation kinetic. As the main oxidant in photo-Fenton reaction is the hydroxyl radical, the oxidation reaction can be represented by Eq. (3)

$$\frac{d[\text{NB}]}{dt} = k[\text{NB}]^\alpha [\bullet\text{OH}]^\beta \quad (3)$$

where: [NB] = concentration of NB at time “*t*” (mg L⁻¹), [•OH] = concentration of hydroxyl radical at time “*t*” (mg L⁻¹), α = the reaction order with respect to NB, β = the reaction order with respect to hydroxyl radical and *k* = overall oxidation rate constant.

Hydroxyl radical produces, in photo-Fenton process, via three ways: (1) the photolysis of hydrogen peroxide to produce one hydroxyl radical (Eq. (4)); (2) the oxidation–reduction reaction between iron solution and hydrogen peroxide (Eq. (5)); (3) the oxidation–reduction of iron solution by means of UV-light (Eq. (6))



However, it is difficult to measure, at specific time, the steady state concentration of hydroxyl radical in aqueous solution. Thus, it is concentration, at specific time, that can be considered constant. Eq. (3) can be rewritten in the form:

$$\frac{d[\text{NB}]}{dt} = k_0[\text{NB}]^\alpha \quad (7)$$

where k_0 = pseudo first-order NB degradation rate constant, i.e. apparent rate constant (min⁻¹). Comparing Eq. (3) with Eq.

(7) indicates that k_0 and *k* are related through the following equation:

$$k_0 = k[\bullet\text{OH}]^\beta \quad (8)$$

Previous works showed that the oxidation kinetic of photo-Fenton reaction can be modelled as a second order, with first order in each concentration of hydroxyl radical and pollutant [32]. Accordingly, Eq. (7) can be reduced to:

$$\frac{d[\text{NB}]}{dt} = k_0[\text{NB}] \quad (9)$$

If Eq. (4) is integrated with initial condition [NB] = [NB]_i for *t* = 0, results

$$\ln \left(\frac{[\text{NB}]_i}{[\text{NB}]} \right) = k_0 t \quad (10)$$

According to Eq. (10), a plot of ln ([NB]_i/[NB]) versus time must lead to a straight lines. Table 2 presents the kinetic data obtained during the oxidation of NB solution (presented data are the average of five experiments performed at the same conditions). A good correlation of the experimental points to a straight line ($R^2 > 0.90$) confirms the validity of the proposed model. Table 2 provides the k_0 values and half-life time for experiments performed at different initial concentrations of H₂O₂ and different initial concentration of Fe(II), different pH and different operational temperature. As it can be noticed, the effect of H₂O₂ on the kinetic constants are higher than Fe(II) effect. As the initial concentration of H₂O₂ was increased from 10 to 35 mg L⁻¹, initial Fe(II) concentration was fixed to 10 mg L⁻¹, the pseudo first-order rate constant was increased from 0.0184 to 0.1228 min⁻¹. As mentioned previously, initial concentration of Fe(II) has a minor effect on NB degradation. This tendency was also observed on the obtained kinetic data; increasing the initial Fe(II) concentration from 10 to 50 mg L⁻¹, at the same initial H₂O₂, was led to no improvement on kinetic constants; the pseudo first-order rate constant was ≈ 0.0524 min⁻¹ at both initial Fe(II) concentrations. Similar tendency was observed with respect to half-life time.

Table 2 also presents the effect of temperature and pH on the NB rate degradation. Trends show that increasing the operational temperature was led to increase on pseudo first-order rate

Table 2
Kinetic data obtained during the oxidation of NB solution by Fenton reaction

Run	[H ₂ O ₂] _i (mg L ⁻¹)	[Fe(II)] _i (mg L ⁻¹)	<i>T</i> (°C)	pH	k_0 (min ⁻¹) (# of samples)	R^2	<i>t</i> _{1/2} (min)
A1	65	10	25	3	0.1228 (5)	97	3
A2	35	10	25	3	0.0524 (5)	95	11
A3	10	10	25	3	0.0184 (5)	98	–
B1	35	20	25	3	0.0540 (4)	96	10
B2	35	30	25	3	0.0563 (4)	96	9.5
B3	35	40	25	3	0.0525 (4)	95	10
B4	35	50	25	3	0.0525 (4)	97	11
C1	35	10	35	3	0.0580 (3)	96	9.5
C2	35	10	45	3	0.060 (5)	96	9
D1	35	10	25	7	0.049 (4)	89	15
D2	35	10	25	9	0.042 (4)	90	22

constant. As the temperature increased from 25 to 45 °C the first-order rate constant, under some other operational temperature, was increased from 0.0524 to 0.060 min⁻¹. The rate of a reaction is a function of temperature (through the rate constant) and concentration. k_0 , the specific reaction rate constant, is given by Arrhenius Eq. (11)

$$k_0 = Ae^{-E/RT} \quad (11)$$

where E = activation energy (J/mol), R = gas constant (J/(mol K)), T = temperature (K) and A = frequency factor.

Experimental results were tested. Eq. (11) was plotted in the form

$$\ln k_0 = \ln A - \frac{E}{RT} \quad (12)$$

A good fit to straight line ($R^2 = 93$) showed that NB oxidation reaction follows Arrhenius equation with E/R value of 644.5 ($E = 5.36$ kJ/mol) and frequency factor of 0.46.

Results in Table 2 also show the significant effect in performing photo-Fenton reaction at acidic condition; at the same operational condition, increasing the solution pH from 3 to 9 was led to decrease in pseudo first-order rate constant from 0.0524 to 0.0420 min⁻¹.

4. Conclusions

The photo-Fenton process shows efficient rule in the degradation and biodegradability improvement of 100 mg L⁻¹ NB solution. Results show that hydrogen peroxide has a good effect in the degradation rate and the bio-compatibility of the organic by-products, 65 mg L⁻¹ of H₂O₂ and 10 mg L⁻¹ Fe(II) during 30 min irradiation time provide 100% NB removal and increase in biodegradability (BOD₅) from 0 up to 34 mg O₂ L⁻¹. Fe(II) catalyst concentration showed small effect in the degradation of NB and the biodegradability improvement. Increasing the initial Fe(II) concentration did not show significant augment in biodegradability (BOD). Increasing the initial iron ion concentrations from 10 to 50 mg L⁻¹ was led to increase in the degradation efficiency and biodegradability from 75 to 90%, for degradation efficiency, and from 13 to 16 for BOD₅. Also, it was noticed that the degradation efficiency and biodegradability increase till they reach a maximum value and then stay stable. Temperature was showed a good effect in NB removal rate and biodegradability enhancement. The treated solutions' acute toxicity was followed, and a considerable reduction of the acute toxicity was observed by photo-Fenton process.

References

- [1] E. Lipczynska-Kochany, Degradation of nitrobenzene and nitrophenols by means of advanced oxidation processes in a homogeneous phase: photolysis in the presence of hydrogen peroxide versus the Fenton reaction, *Chemosphere* 24 (1992) 1369–1380.
- [2] EPA site, visited on April 2002, www.scorecard.org/chemical-groups/one-list.td?short_list_name=pp.
- [3] K. Hayward, Drinking water contaminant hit-list for US EPA, *Water* 21 (1999) 4.
- [4] J. Duguet, C. Anselme, P. Mazounie, J. Mallevalle, Application of combined ozone-hydrogen peroxide for the removal of aromatic compounds from a ground water, *Ozone Sci. Eng.* 12 (1989) 281g–284g.
- [5] P.H. Howard, *Handbook of Environmental Fate and Exposure Data for Organic Chemical, Large Production and Priority Pollutants*, vol. I, Lewis Publishers, Chelsea, Michigan (USA), 1989.
- [6] H. Loebel, G. Stein, J. Weiss, Hydroxylation of nitrobenzene, *J. Chem. Soc.* (1949) 2704–2709.
- [7] Metcalf and Eddy Inc., *Wastewater Engineering: Treatment, Disposal and Reuse*, third ed., Mc Graw-Hill, New York, USA, 1985 (Spanish version).
- [8] M. Davis, J. Turley, D. Casserly, R. Guthrie, Partitioning of selected organic pollutants in aquatic ecosystems, in: T. Oxley, S. Barry (Eds.), *Biodeterioration*, vol. 5, pp. 176–184.
- [9] B. Zoeteman, K. Harmsen, J. Linders, C. Morra, W. Sloof, Persistent organic pollutants in river water and ground water of the Netherlands, *Chemosphere* 9 (1980) 231–249.
- [10] R.J. Stephenson, S. Duff, Coagulation and precipitation of a mechanical pulping effluent. Part II: toxicity removal and metal salt recovery, *Water Res.* 30 (4) (1996) 793–798.
- [11] M.J. Rosa, M.N. de Pinho, The role of ultrafiltration and nanofiltration on the minimisation of the environmental impact of bleached pulp effluents, *J. Membr. Sci.* 102 (1995) 155–161.
- [12] A.G. Werker, E.R. Hall, Limitations for biological removal of resin acids from pulp mill effluent, *Water Sci. Technol.* 40 (11–12) (1999) 281–288.
- [13] F. Al-Momani, E. Tourauda, J.R. Degorce-Dumas, J. Roussy, O. Thomas, Biodegradability enhancement of textile dyes and textile wastewater by VUV photolysis, *J. Photochem. Photobiol. A Chem.* 153 (2002) 1–3.
- [14] E. Chamarro, A. Marco, S. Esplugas, Use of Fenton reagent to improve organic chemical biodegradability, *Water Res.* 35 (4) (2001) 1047–1051.
- [15] S. Contreras, M. Rodríguez, E. Chamarro, S. Esplugas, J. Casado, Oxidation of nitrobenzene by O₃/UV: the influence of H₂O₂ and Fe(III). Experiences in a pilot plant, *Water Sci. Technol.* 44 (2001) 39–46.
- [16] M.R. Hoffman, S.T. Martin, W. Choi, D.W. Bahnemann, Environmental applications of semiconductor photocatalysis, *Chem. Rev.* 95 (1995) 69–96.
- [17] A. Marco, S. Esplugas, G. Saum, How and why to combine chemical and biological processes for wastewater treatment, *Water Sci. Technol.* 35 (4) (1997) 321–327.
- [18] G.B. Raupp, C.T. Junio, Photocatalytic oxidation of oxygenated air toxics, *Appl. Surf. Sci.* 72 (1993) 321–327.
- [19] S. Hager, R. Bauer, Heterogeneous photocatalytic oxidation of organics for air purification by near UV irradiated titanium dioxide, *Chemosphere* 38 (7) (1999) 1549–1559.
- [20] F.J. Beltrán, J.F. García-Araya, J. Frades, P. Alvarez, O. Gimeno, Effects of single and combined ozonation with hydrogen peroxide or UV radiation on the chemical degradation and biodegradability of debittering table olive industrial wastewater, *Water Res.* 33 (3) (1999) 723–732.
- [21] F.J. Benitez, J.L.R. Acero, J. Francisco, J. Garcia, Kinetics of photodegradation and ozonation of pentachlorophenol, *Chemosphere* 51 (2003) 651–662.
- [22] W.H. Glaze, J.W. Kang, D.H. Chapin, The chemistry of water treatment processes involving ozone, hydrogen peroxide and ultraviolet radiation, *Ozone Sci. Eng.* 9 (4) (1987) 335–342.
- [23] F.J. Beltran, J.M. Encinar, M.A. Alonso, Nitroaromatic hydrocarbon ozonation in water. Part 2: combined ozonation with hydrogen peroxide or UV radiation, *Ind. Eng. Chem. Res.* 37 (1998) 32–40.
- [24] H. Gulyas, Processes for the removal of recalcitrant organics from industrial Wastewater, *Water Sci. Technol.* 36 (1997) 9–16.
- [25] F. Al-Momani, C. Sans, S. Esplugas, A comparative study of the advanced oxidation of 2,4-dichlorophenol, *J. Hazard. Mater.* B107 (2004) 123–129.
- [26] L.J. Heidt, G.W. Tregay, F.A. Middleton, Influence of the pH upon the photolysis of the uranyl oxalate actinometer system, *J. Phys. Chem.* 74 (1979) 1876–1882.
- [27] S. Esplugas, M. Vicente, Calibrado del fotorreactor anular, *Afinidad* 40 (1983) 453–457.

- [28] Standard methods for the examination of water and wastewater, 16th ed., American Public Health Association, American Water Works Association, Water Pollution Control Federation, 1985.
- [29] M.Y. Ghaly, G. Hartel, R. Mayer, R. Haseneder, Photochemical oxidation of *p*-chlorophenol by UV/H₂O₂ and photo-Fenton process: a comparative study, *Water Manage.* 21 (2001) 41–47.
- [30] J. De Laat, H. Gallard, Catalytic decomposition of hydrogen peroxide by Fe(III) in homogeneous aqueous solution: mechanism and kinetic modeling, *Environ. Sci. Technol.* 33 (1999) 2726–2732.
- [31] A.P. Murphy, W.J. Boegli, M.K. Price, C.D. Moody, A Fenton-like reaction to neutralize formaldehyde waste solutions, *Environ. Sci. Technol.* 23 (1989) 166–169.
- [32] W.H. Glaze, J.W. Kang, Advanced oxidation processes: test of a kinetic model for the oxidation of organic compounds with ozone and hydrogen peroxide in a semibatch reactor, *Ind. Eng. Chem. Res.* 28 (11) (1989) 1580–1587.